Electronic Supplementary Information

New ternary iron(III) aminobisphenolate hydroxyquinoline complexes as potential therapeutic agents

Cristina P. Matos[1#], Yasemin Yildizhan[2#], Zelal Adiguzel[2#], Fernando R. Pavan[3], Débora L. Campos,[3] Joao Costa Pessoa[1], Liliana P. Ferreira,[5,6] Ana Isabel Tomaz,[4] Isabel Correia[1]*, Ceyda Acilan[7*]

[1]Centro de Química Estrutural, Instituto Superior Técnico, Universidade de Lisboa, Av. Rovisco Pais 1, 1049-001, Lisbon, Portugal
[2]TUBITAK, Marmara Research Center, Genetic Engineering and Biotechnology Institute, Gebze/Kocaeli, Turkey
[3]Faculdade de Ciências Farmacêuticas, UNESP, C.P.582, Araraquara, SP 14801-902, Brazil
[4]Centro de Química Estrutural, Faculdade de Ciências, Universidade de Lisboa, Campo Grande, 1749-016 Lisbon, Portugal
[5]BioISI, Faculdade de Ciências, Universidade de Lisboa, Campo Grande, 1749-016 Lisbon, Portugal
[6]Department of Physics, University of Coimbra, 3004-516 Coimbra, Portugal
[7]Koc University, School of Medicine, Sariyer, Istanbul, Turkey

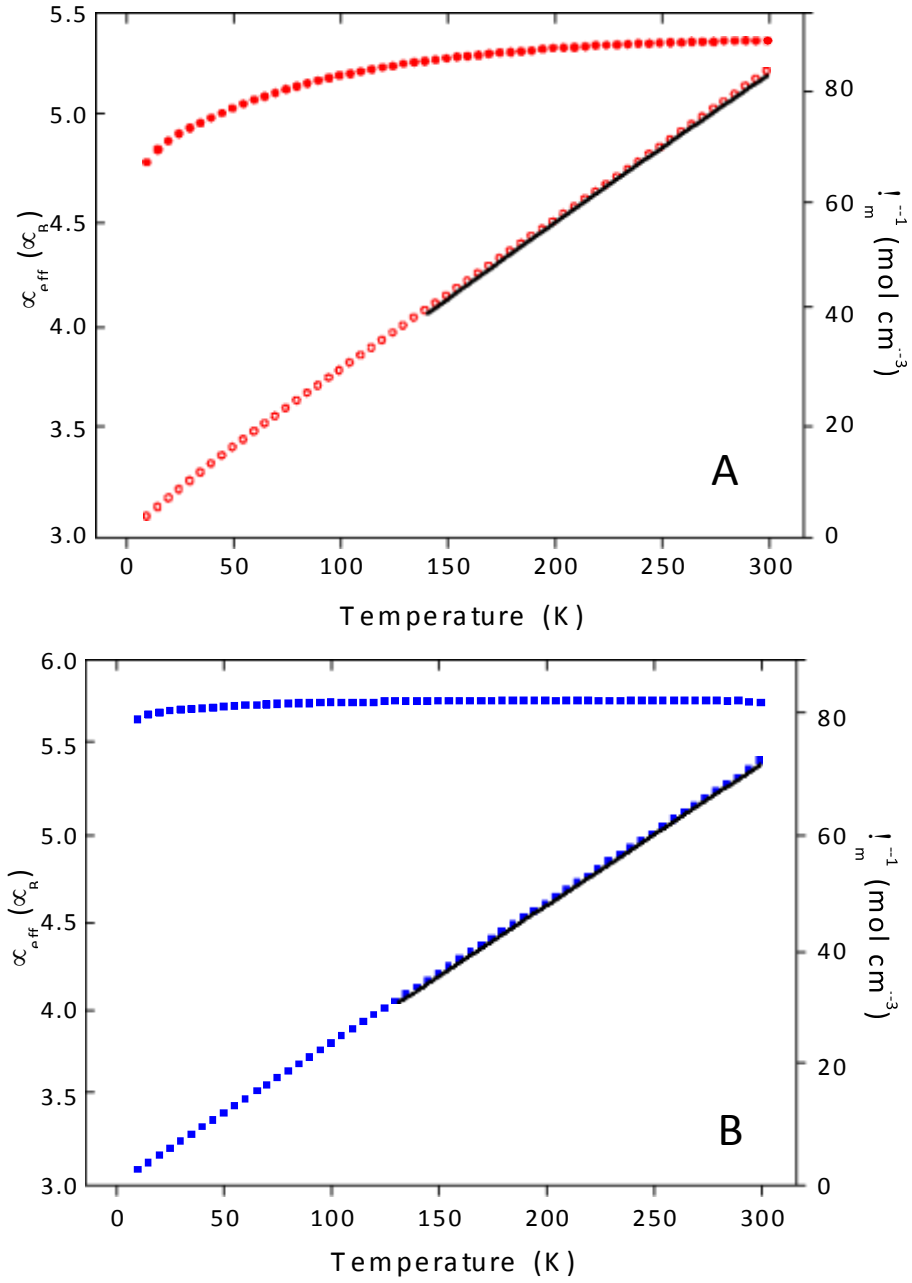

Figure S1 - Magnetization measurements: thermal variation of the effective magnetic moment, μ_{eff}, (closed symbols) and of the inverse molar susceptibility, χ_m^{-1}, (open symbols) obtained from the magnetization *vs.* temperature measurements of complex 1 (*A*) and of complex 2 (*B*). Data fit to a modified Curie law, $\chi=C/T+k$, *C* being the Curie constant, related to μ_{eff} by $C=(N_A\mu_{eff}^2)/(3k_B)$ (where N_A is the Avogadro number and k_B is the Boltzmann constant) and *k* is also a constant. The results obtained from the fittings (R^2=0.999) were: $\mu_{eff}=5.31\ \propto_B$ and $k=1.4(3)\times10^{-5}$ $cm^3\ mol^{-1}$ for 1 (red) and $\mu_{eff}=5.81\ \propto_B$ and $k=-3.4(2)\times10^{-5}$ $cm^3\ mol^{-1}$ for 2 (blue), in accordance with the effective magnetic moment expected for High Spin Fe(III) d5 centers.

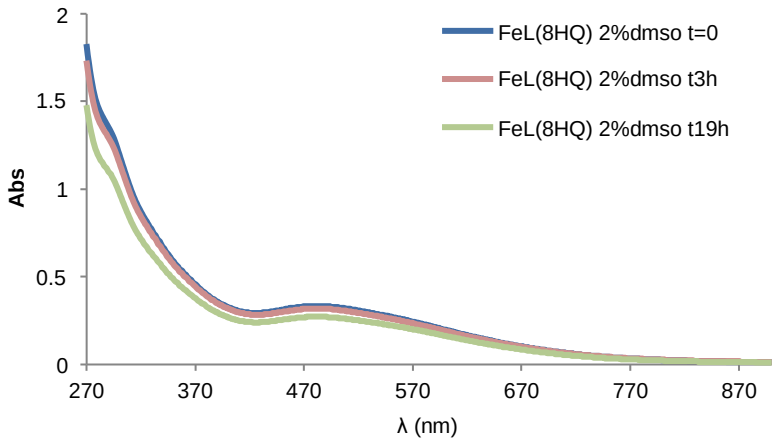

Figure S2- UV-Vis absorption electronic spectra measured for complex 1 [Fe(L)(8HQ)] at a concentration of ~125 µM in 2% DMSO-H_2O solution recorded over time. After 3 hours the complex maintains its structure and is mostly in solution; the complex precipitation is visually noticeable after 19 hours. The pH of the solution is 7.38.

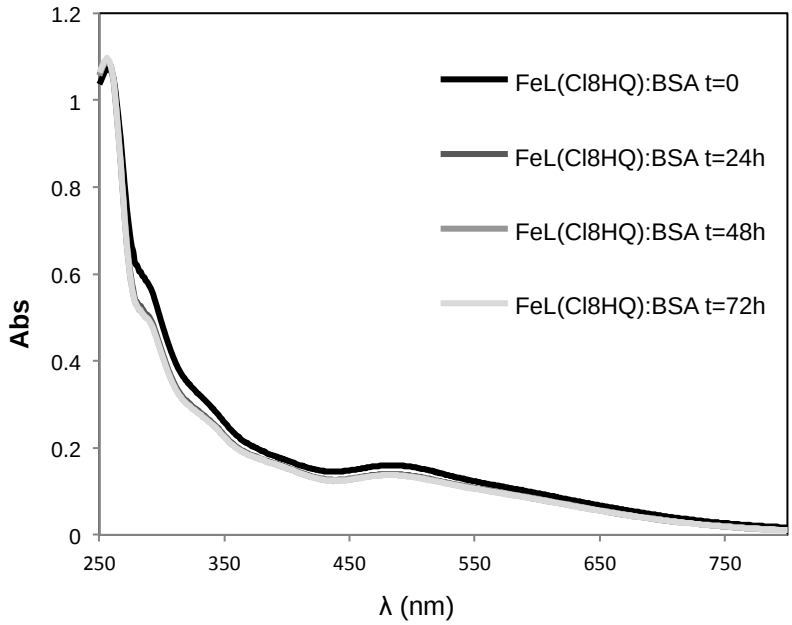

Figure S3 - UV-Vis absorption electronic spectra measured for complex (2) [FeL(Cl8HQ)] (31.5 µM) in the presence of BSA (34.2 µM) recorded over time in 5%DMSO/buffer (NH_4HCO_3 25mM, pH 7.4). No changes in the spectrum pattern and no precipitation was macroscopically observed, supporting that the complex maintains its structural integrity up to at least 72 h.

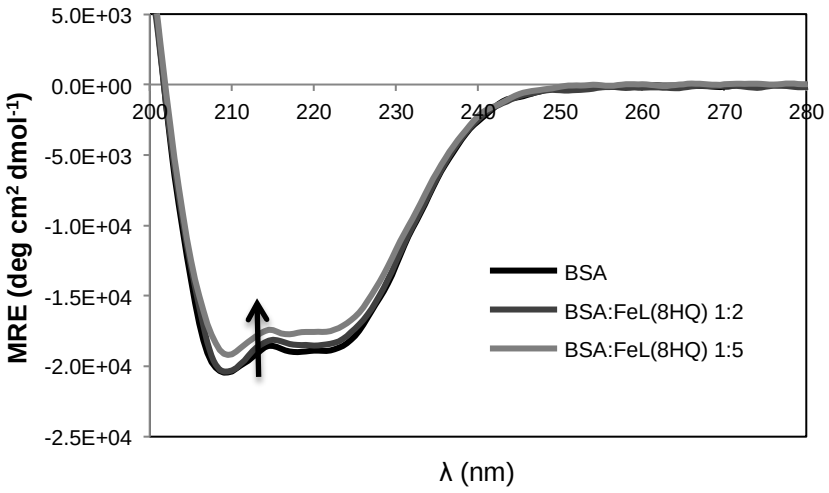

Figure S4 – Far UV-Vis CD spectra for BSA (1.2 µM) in the absence and presence of different concentrations of complex 1 [Fe(L)(8HQ)]; BSA:complex mixtures were measured after 3 h incubation time at room temperature. The complex induces changes in the protein helicity at higher complex:protein ratios.

Table S1 – Binding of iron complexes to BSA in methanol/pH7 buffer (NH_4HCO_3 25mM, pH 7.4): α-helical (%) content of BSA calculated from the far-UV protein spectrum in the absence and presence of iron complexes 1 and 2, formulated as [Fe(L)(8HQ)] and [Fe(L)(Cl8HQ)], respectively (protein:complex molar ratio is indicated in each case).

Sample	α-Helix (%) [a] (λ = 208 nm)	α-Helix (%) [a] (λ = 222 nm)
BSA	83	70
BSA:[Fe(L)(8HQ)] 1:2	82 (←1%)	69 (←2%)
BSA:[Fe(L)(8HQ)] 1:5	77 (←7%)	66 (←4%)
BSA	80	67
BSA:[Fe(L)(Cl8HQ)] 1:2	80	68 (→1%)
BSA:[Fe(L)(Cl8HQ)] 1:5	81 (→1%)	68 (→1%)

[a]The α- helical content (%) was calculated from the MRE values at 208 or 222 nm, using the following equaSons (respecSvely):

α-Helix (%) = $-(MRE_{208}-4000)/(3300-4000)*100$

α-Helix (%) = $-(MRE_{222}-2340)/30300*100$

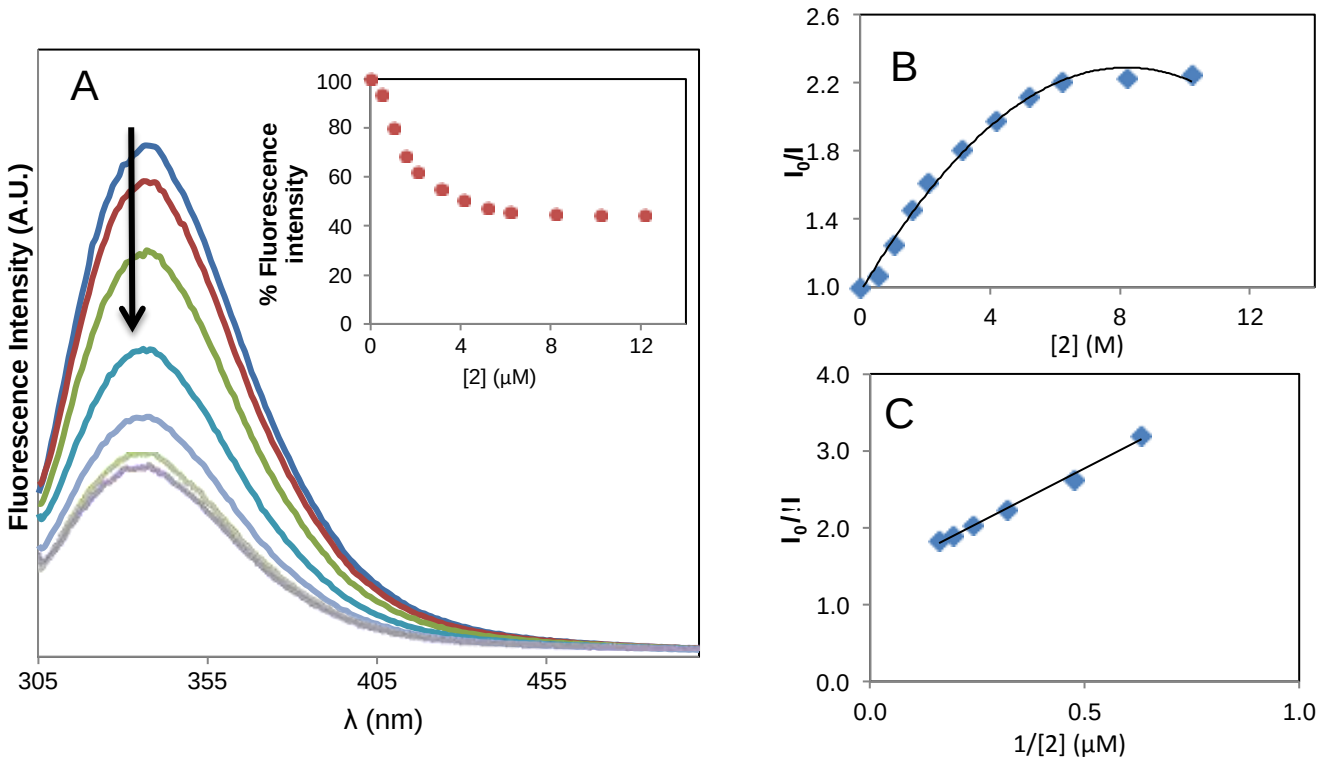

Figure S5 – A) Fluorescence emission spectra recorded at room temperature for solutions containing HSA (2.1 μM) and increasing amounts of 2 (0.5 – 8.2 μM), in DMSO-NH_4HCO_3 25mM, pH 7.4. As the amount of complex increases the fluorescence intensity of HSA is significantly quenched (~55 % quenching, as shown in the inset). B) Stern-Volmer plot for the fluorescence quenching of HSA shown in A) showing a downward curvature typical for the case of two fluorophores, one accessible and the other inaccessible to the quencher (R^2 = 0.992). C) Plot for the quenching of HSA in the presence of complex 2 obtained taking into account the accessible fraction of the tryptophan fluorophore calculated with equation 6 (R^2 = 0.993).

The Stern-Volmer plot for the HSA-2 interaction is not linear but is well-fitted by a quadratic equation with a downward curvature. This behavior is usually related with the existence of two distinct fluorophore populations (in this case Trp214) in solution[1] where one of them is more accessible to the quencher than the other. Indeed, the number of binding sites obtained per HSA molecule was 1.4, thus on average more than one binding site might be available for the binding of 2, in accordance with the Stern-Volmer results. In this case, a rearrangement of the Stern-Volmer equation to consider the fractional accessibility of the fluorophore can be used:

$$\frac{I_0}{\Delta I} = \frac{1}{([Q]\, f_a\, K_{SV})} + \frac{1}{f_a}$$

where $\Delta I = I_0 - I$, is the decrease in the fluorescence observed, f_a is the accessible fluorophore fraction and K_{SV} is the Stern–Volmer quenching constant for the accessible tryptophan fraction. A plot of $I_0/\Delta I$ versus [Q] should be linear and K_{SV} can thus be obtained (Fig. S6C). Using this approach, we calculated that only 75% of albumins' Trp214 was accessible to the iron complex. Since HSA has only one Trp residue this is probably related to the existence of different protein conformations with different accessibilities to the fluorophore,[2] as previously observed also by us.[3]

1– W. R. Lakowicz, *Principles of Fluorescence Spectroscopy*, Springer, 3rd edn., 2006.
2 – S. Tardioli, I. Lammers, J. H. Hooijschuur, F. Ariese, G. van der Zwan and C. Gooijer, *J. Phys. Chem. B*, 2012, 116, 7033--7039.
3 – N. Ribeiro, R. E. Di Paolo, A. M. Galvao, F. Marques, J. C. Pessoa and I. Correia, *Spectrochim. Acta A*, 2018, 204, 317--327.

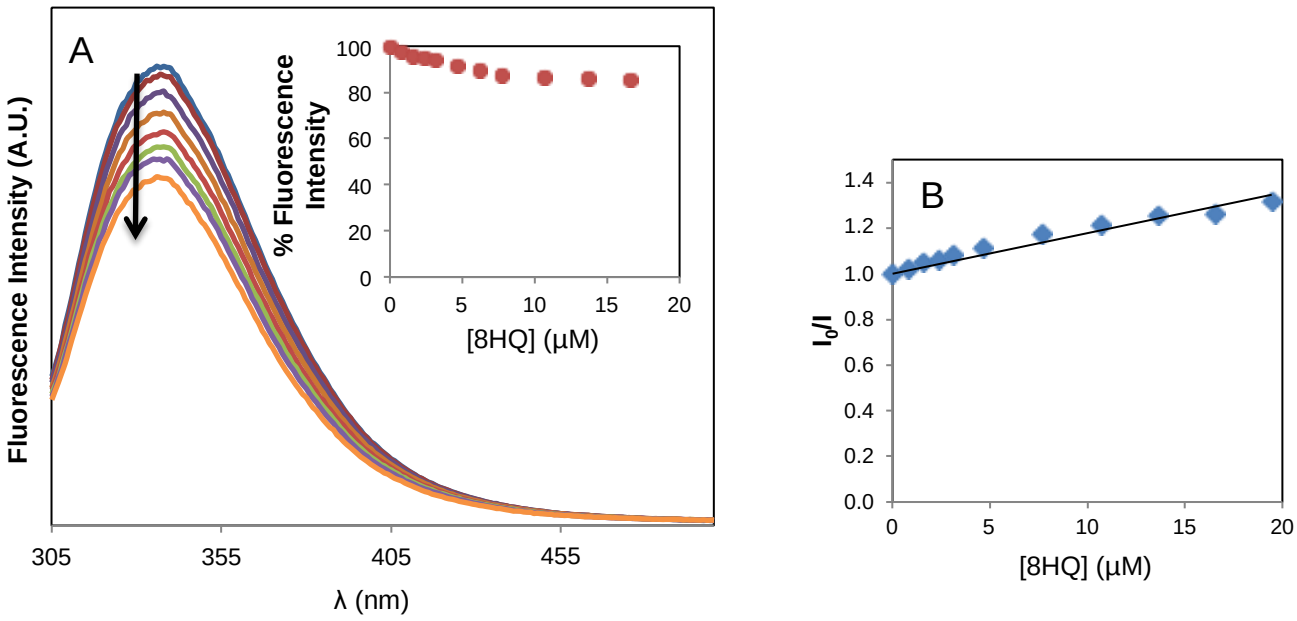

Figure S6 – A) Fluorescence emission spectra recorded at room temperature for solutions containing HSA (2.1 μM) and increasing amounts of 8HQ (0.8 – 19 μM), in DMSO-NH_4HCO_3 25mM, pH 7.4. As the concentration of 8HQ increases the emission intensity of HSA is slightly quenched (~15 % quenching at λ_{em}^{max} = 336 nm, as shown in the inset). B) Stern-Volmer plot for the fluorescence quenching of HSA shown in A) (R^2 = 0.943).

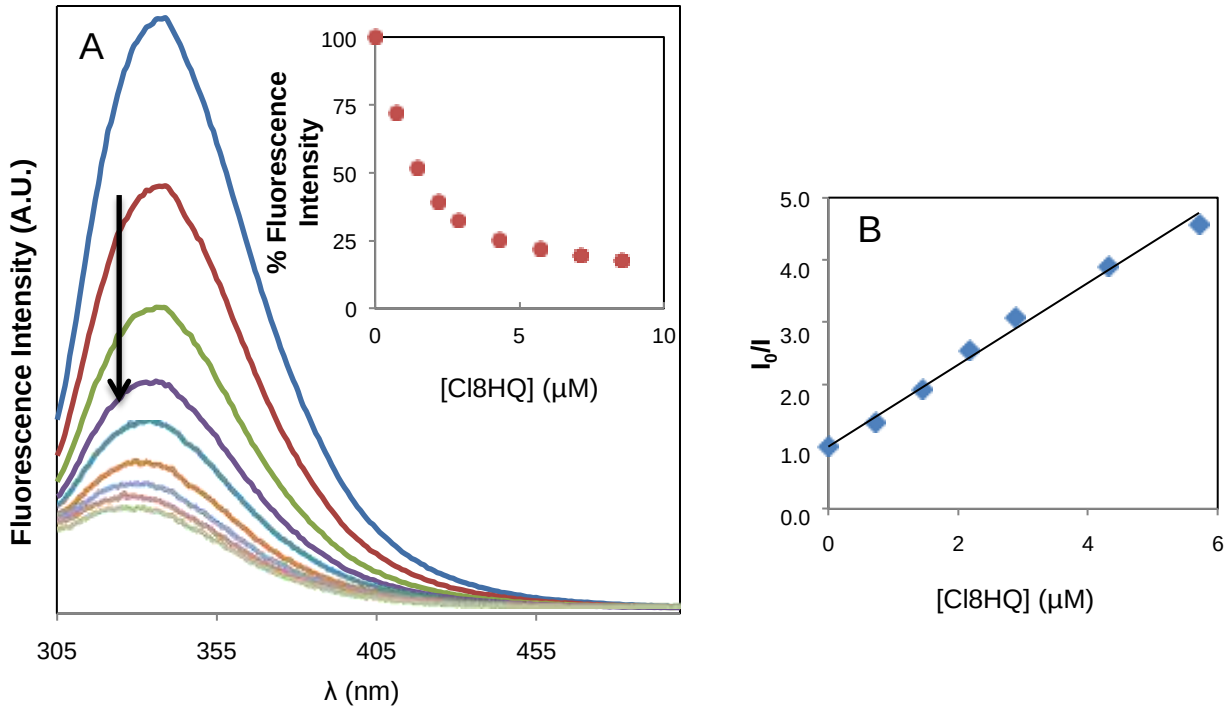

Figure S7 – A) Fluorescence emission spectra recorded at room temperature for solutions containing HSA (2.2 μM) and increasing amounts of Cl8HQ (0.7 – 8.5 μM, increasing in the arrow direction), in DMSO-NH_4HCO_3 25mM, pH 7.4. As the concentration of Cl8HQ increases the fluorescence intensity of HSA is significantly quenched (~ 82 % quenching at λ_{em}^{max} = 337 nm, as shown in the inset). B) Stern-Volmer plot for the fluorescence quenching of HSA shown in A) (R^2 = 0.991).

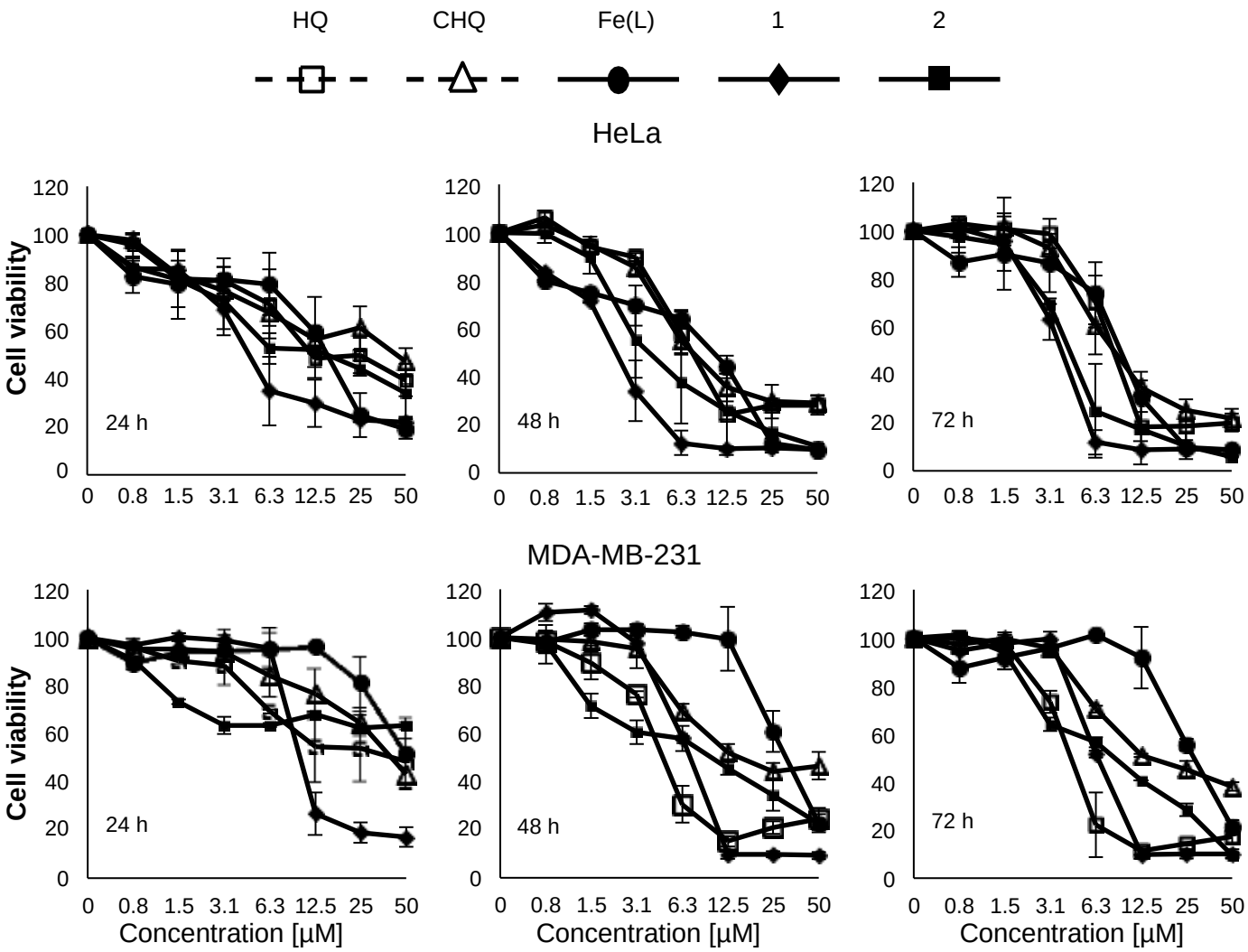

Figure S8 - Cytotoxicity of the compounds under study: dose-response curves obtained for cells treated with the complexes indicated; cell viability was measured at 24, 48 and 72 h. IC_{50} values calculated are summarized in Table 5.

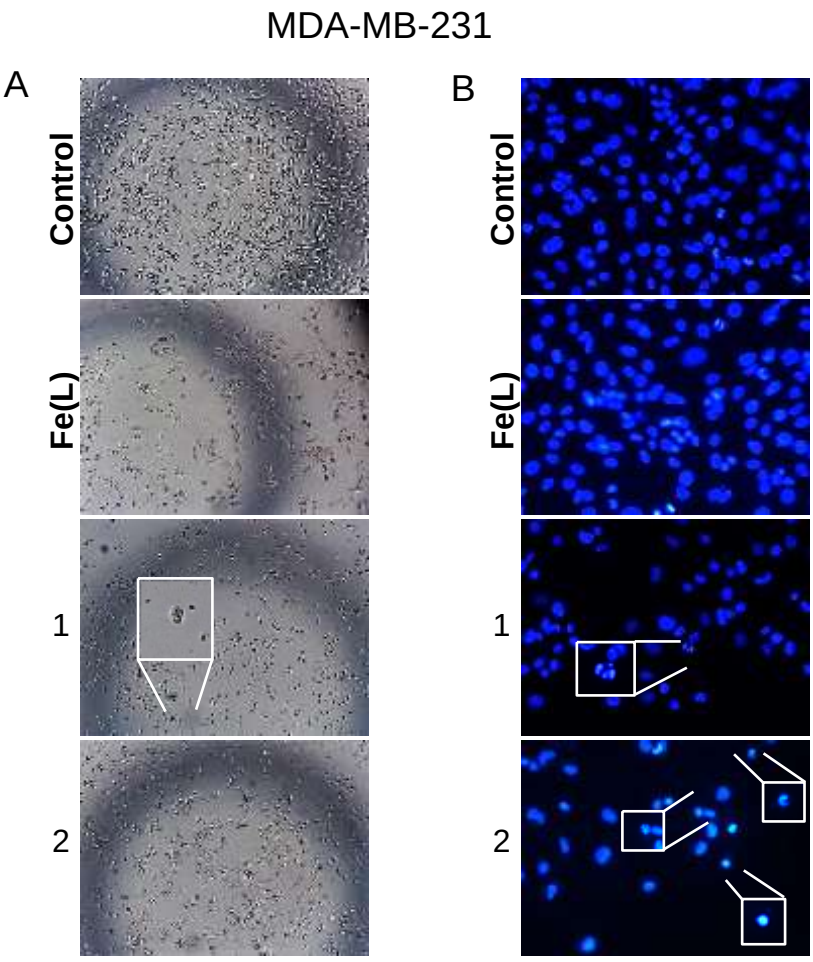

Figure S9 - Representative images of MDA-MB-231 cells showing A) cellular shrinkage and blebbing and B) DNA condensation and fragmentation at 24 h, 12.5 µM treatment. Insets indicate enlarged views of such morphologies.

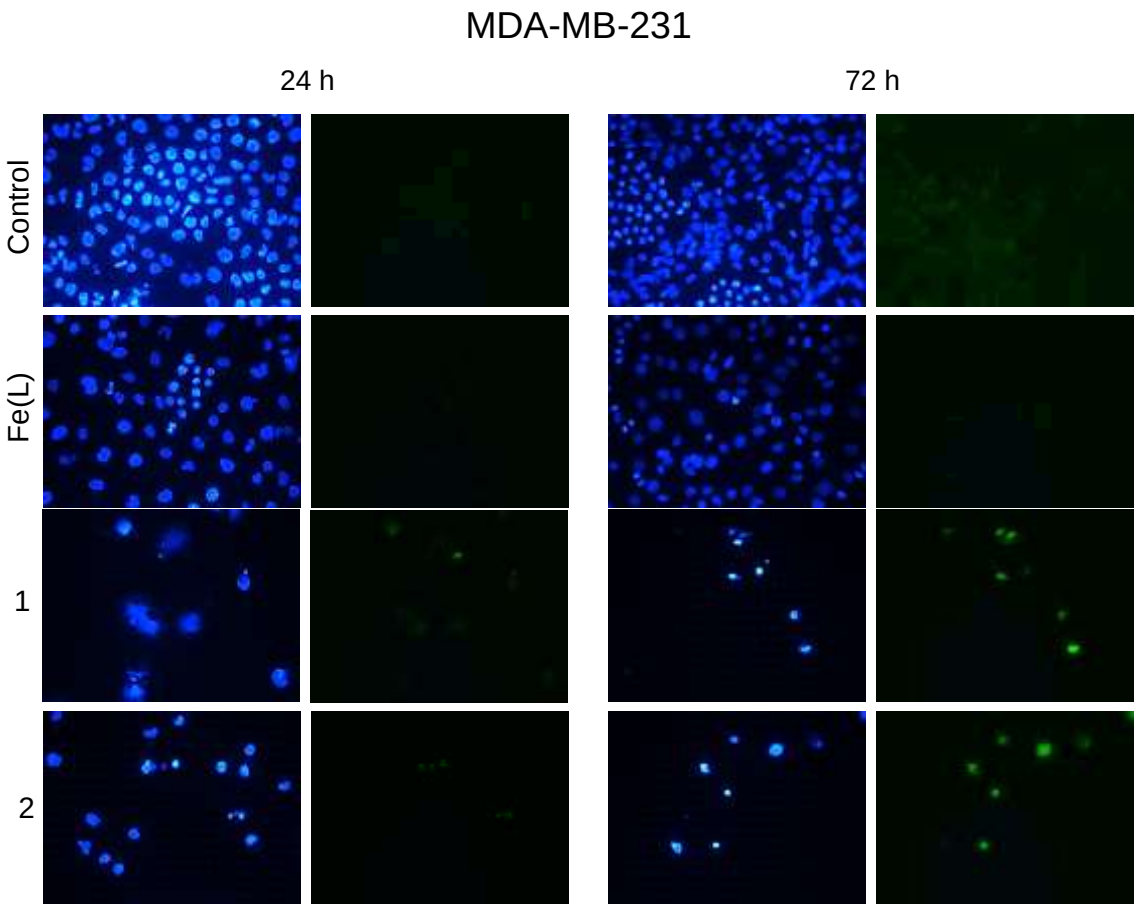

Figure S10 - Representative images of MDA-MB-231 cells showing DNA morphology (blue) and TUNEL (green) positivity at 24 and 72 h, upon 12.5 µM treatment.

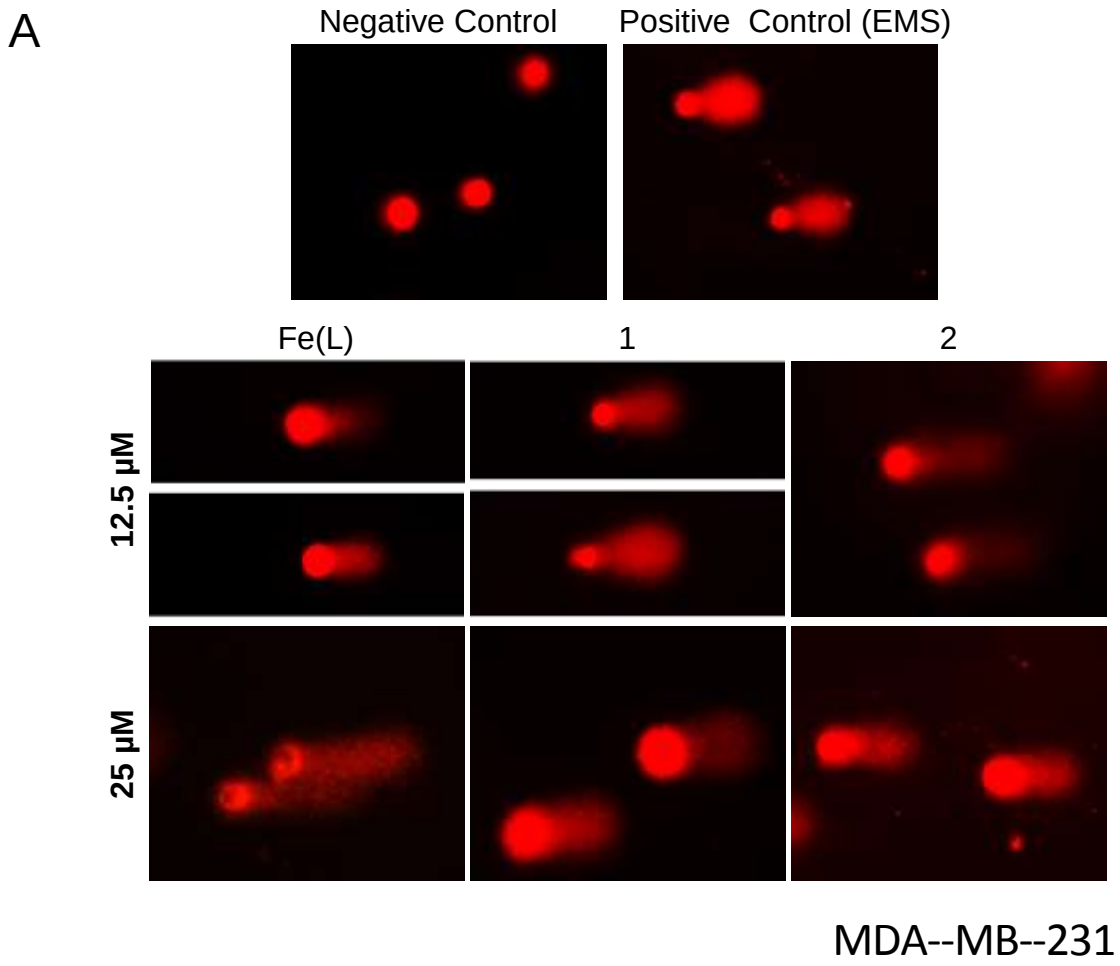

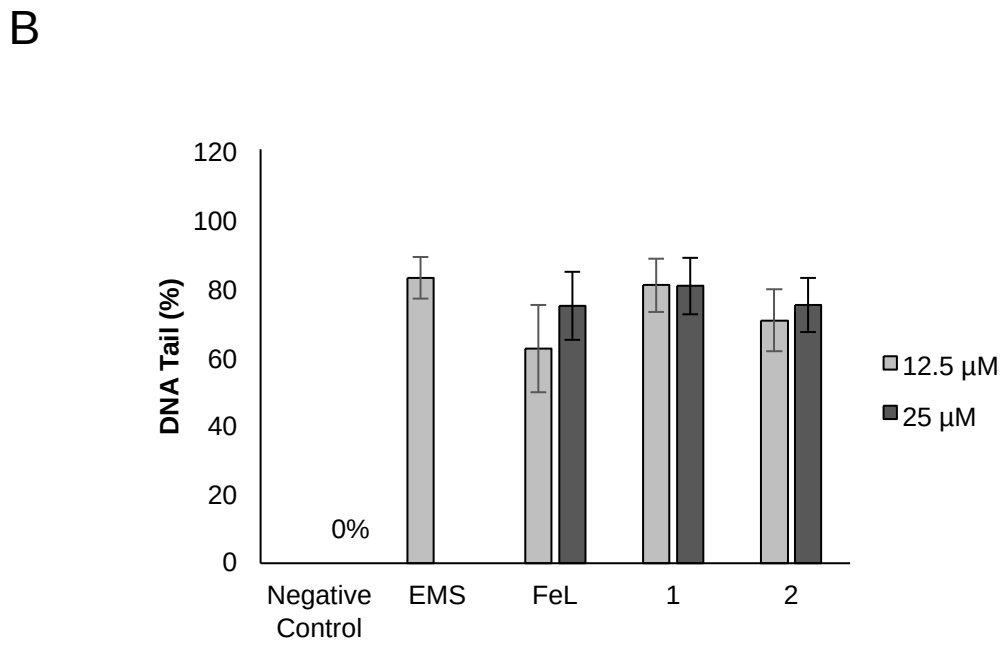

Figure S11, - COMET assay in MDA-MB-231 line. A) Negative control: DMEM/F12 treated cells, Positive control: EMS treated cells. Representative images of nuclei of MDA-MB-231 cells treated with Fe(L), 1 or 2 for 24 h, 12.5 and 25 µM treatment. B) Quantification of tail lengths of cells shown in A).